



# Heartbeat Interval Error Compensation Method for Low Sampling Rates Photoplethysmography Sensors

Watanabe, Kento  
Izumi, Shintaro  
Yano, Yuji  
Kawaguchi, Hiroshi  
Yoshimoto, Masahiko

---

(Citation)

IEICE Transactions on Communications, E103.B(6):645-652

(Issue Date)

2020-06

(Resource Type)

journal article

(Version)

Version of Record

(Rights)

© 2020 The Institute of Electronics, Information and Communication Engineers

(URL)

<https://hdl.handle.net/20.500.14094/90007349>





## **on Communications**

**VOL. E103-B NO. 6  
JUNE 2020**

**The usage of this PDF file must comply with the IEICE Provisions on Copyright.**

**The author(s) can distribute this PDF file for research and educational (nonprofit) purposes only.**

**Distribution by anyone other than the author(s) is prohibited.**

**A PUBLICATION OF THE COMMUNICATIONS SOCIETY**



**The Institute of Electronics, Information and Communication Engineers  
Kikai-Shinko-Kaikan Bldg., 5-8, Shibakoen 3chome, Minato-ku, TOKYO, 105-0011 JAPAN**

# Heartbeat Interval Error Compensation Method for Low Sampling Rates Photoplethysmography Sensors\*

Kento WATANABE<sup>†</sup>, Nonmember, Shintaro IZUMI<sup>†a)</sup>, Member, Yuji YANO<sup>†</sup>, Nonmember, Hiroshi KAWAGUCHI<sup>†</sup>, Member, and Masahiko YOSHIMOTO<sup>†</sup>, Fellow

**SUMMARY** This study presents a method for improving the heartbeat interval accuracy of photoplethysmographic (PPG) sensors at ultra-low sampling rates. Although sampling rate reduction can extend battery life, it increases the sampling error and degrades the accuracy of the extracted heartbeat interval. To overcome these drawbacks, a sampling-error compensation method is proposed in this study. The sampling error is reduced by using linear interpolation and autocorrelation based on the waveform similarity of heartbeats in PPG. Furthermore, this study introduces two-line approximation and first derivative PPG (FDPPG) to improve the waveform similarity at ultra-low sampling rates. The proposed method was evaluated using measured PPG and reference electrocardiogram (ECG) of seven subjects. The results reveal that the mean absolute error (MAE) of 4.11 ms was achieved for the heartbeat intervals at a sampling rate of 10 Hz, compared with 1-kHz ECG sampling. The heartbeat interval error was also evaluated based on a heart rate variability (HRV) analysis. Furthermore, the mean absolute percentage error (MAPE) of the low-frequency/high-frequency (LF/HF) components obtained from the 10-Hz PPG is shown to decrease from 38.3% to 3.3%. This error is small enough for practical HRV analysis.

**key words:** error compensation, heartbeat, heart rate variability analysis, sampling error, photoplethysmography (PPG)

## 1. Introduction

Daily health monitoring is useful for preventing lifestyle diseases, such as cardiovascular diseases, because it raises health awareness, and lead to improved lifestyle habits [1]. Wearable healthcare devices are important for monitoring daily health. For daily health monitoring, there are various important indicators (e.g. heartbeat, blood pressure, and blood glucose level). Among these indicators, heartbeat is considered a useful biosignal for heart disease detection, exercise intensity estimation [2], and heart rate variability (HRV) analysis [3], [4]. It has been reported that heart rate variability analysis (HRVA) can recognize fatigue and stress conditions [5], and drowsiness and diseases arising from these conditions [6]. For practical use, it is necessary to measure heart rates accurately over a long period. Typically, heartbeat intervals are acquired using electrocardiography (ECG) and photoplethysmography (PPG) [7]. These

heartbeat intervals are calculated as R-to-R interval (RRI) of ECG and peak-to-peak interval (PPI) of PPG.

Although ECG can yield more accurate heartbeat intervals, because it directly measures the potential difference on the body surface attributable to the electrical excitation of the heart, it is not suitable for long-term use, because it requires multiple electrodes to be directly attached to the body [8].

In contrast, PPG sensors can efficiently measure heartbeat without electrodes. It irradiates the body's surface with green or red light, and measures the amount of light absorption by hemoglobin as created by changes in blood volume [9], [10]. There is a few millisecond difference between the heartbeat arrival time of ECG and PPG, because PPG has propagation delay in the blood vessel [11]. However, this difference is not a problem in most applications. Therefore, PPG can easily be implemented in wearable devices such as smartphones, smart bands, and smart rings [12]–[14]. Because the size of the wearable sensors and their battery capacity are strictly limited, it is necessary to reduce power consumption.

There are two major power-consuming components in PPG sensors: LEDs and a wireless data communication circuit (e.g. Bluetooth Low Energy). An effective way of reducing their power consumption is to reduce the activity rate of the LEDs and the amount of transmission data by lowering the sampling rate. However, this leads to a large time error in the extracted heartbeats because of the sampling error; the minimum sampling rate and power reduction efficiency are determined based on the heartbeat accuracy interval required by the application. For instance, an application utilizing heartbeat fluctuation, such as heart rate variability analysis [3], requires that the time error in the heartbeat interval does not exceed a few milliseconds.

To overcome the drawback of sampling-rate reduction methods, we propose an error compensation method based on linear interpolation and autocorrelation using waveform similarity. A preliminary version of this study has been reported in the literature [15]. Although the preliminary study focused on ECG in the performance evaluation, we focus on PPG in this study, because the power consumption of PPG can be reduced more efficiently by sampling rate reduction. Furthermore, this study presents additional error reduction methods; each method is evaluated in detail using seven subjects.

The rest of this paper is structured as follows. Sec-

Manuscript received July 16, 2019.

Manuscript revised October 16, 2019.

Manuscript publicized December 25, 2019.

<sup>†</sup>The authors are with the Graduate School of System Informatics, Kobe University, Kobe-shi, 657-8501 Japan.

\*This paper is based on the results obtained from a project commissioned by the New Energy and Industrial Technology Development Organization (NEDO).

a) E-mail: shin@godzilla.kobe-u.ac.jp

DOI: 10.1587/transcom.2019HMP0002

tion 2 presents the overview of conventional sampling-rate reduction methods for PPG sensors. The proposed sampling error compensation methods are described in Sect. 3. Section 4 presents the experiment results of the proposed methods, which are discussed in Sect. 5. Finally, the conclusions are presented in Sect. 6.

## 2. Sampling-Rate Reduction Methods for PPG

As mentioned in Sect. 1, reducing the sampling rate is important for reducing the power consumption in PPG sensors. The simplest method is to reduce the overall sampling rate, as shown in Fig. 1(a). Other low sampling-rate-sensing techniques for PPG sensors have been proposed [16], [17].

A parabola approximation method [18] is evaluated to mitigate the sampling error at low sampling rates (see Fig. 1(a)). It is reported that 20-Hz sampled peaks using parabola approximation are comparable to 250-Hz sampled reference signal peaks.

One proposed method uses compressed sampling (CS) technology to reduce the sampling rate to below the Nyquist frequency (see Fig. 1(b)) [16]. The CS method assumes that the PPG signal is sparse in the frequency domain, and performs signal reconstruction on the data of a small number of sample points using matrix operation. In health monitoring applications, the signal reconstruction process can be performed using a server or a gateway (e.g. a smart phone), and the power consumption required for calculation is negligible. However, in this method, because it is impossible to fully reconstruct the original signal, the heartbeat interval error becomes large, resulting in reduced reliability.

In literature [17], a method that samples only the signal around the peak of the PPG waveform to obtain the heartbeat interval is proposed (see Fig. 1(c)). First, two beats extracted from the PPG waveform are sampled to obtain one heartbeat interval. Based on the obtained heartbeat interval, the timing of the detection of the peak of the next PPG waveform is estimated. Sampling commences before

the peak, and when the peak is detected, sampling is terminated. Then, the timing of the next peak is estimated again. By restricting the sampling to the vicinity of the peak in this method, the PPG sensor significantly reduces the activity rate of the LED which consumes most of the power. On the other hand, when this method fails to detect a peak, it is necessary to repeat the entire process, and power consumption increases. In particular, the peak detection may fail due to a body motion artifact or arrhythmias, such as extrasystoles, which may occur even in healthy subjects [19].

## 3. Proposed Sampling Error Compensation Method for Heartbeat Interval Acquisition

Although reducing the sampling rate effectively contributes to power consumption reduction, the heartbeat interval error increases according to the sampling error. Figure 2 shows the PPG waveforms sampled respectively at 1 kHz and 20 Hz. This graph indicates that the interval between peaks, i.e., the heartbeat interval has a large time error corresponding to low sampling rates.

In this study, we propose a sampling error compensation method for the ultra-low sampling-rate condition by incorporating interpolation and autocorrelation into the simple sampling-rate reduction method shown in Fig. 1(a). The proposed method exploits the periodicity and similarity of the heartbeat waveform in PPG. In addition, a waveform-similarity improvement method using the peak waveform approximation and waveform transform is introduced.

### 3.1 Heartbeat Interval Error Compensation Using Linear Interpolation and Autocorrelation

As shown in Fig. 2, the sampling rate reduction increases the sampling error and decreases the accuracy of the extracted heartbeat interval. Generally, the heartbeat interval is calculated from the peak-to-peak interval of the PPG. In contrast, we introduce a heartbeat interval extraction algorithm based on the similarity of the heartbeat shapes.

Figure 3 shows the flowchart of the proposed method. First, we receive the data sampled by the PPG sensor at a low sampling rate ( $F_s$ ). Next, the peak of the signal is detected, and linear interpolation and resampling are performed at 1 kHz. The peaks detected at this point are

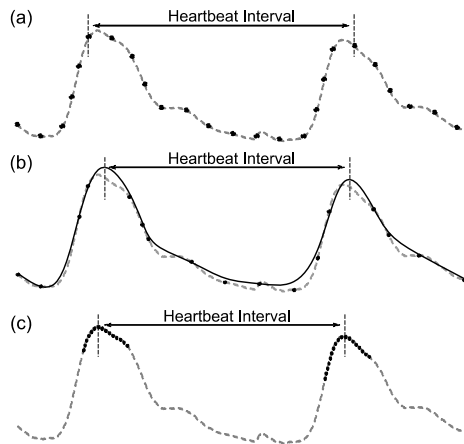


**Fig. 1** Overview of conventional heartbeat sensing methods at low sampling rates; (a) sampling rate reduction, (b) compressed sampling, (c) heartbeat locked loop.

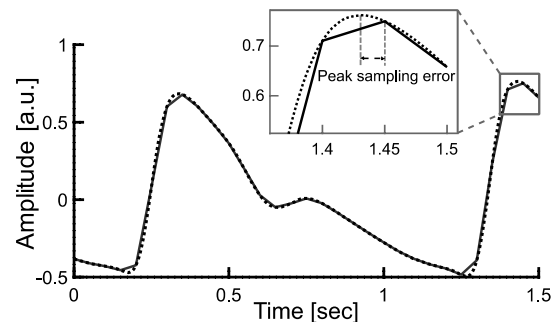


**Fig. 2** Example of PPG waveform at 1 kHz and 20 Hz.

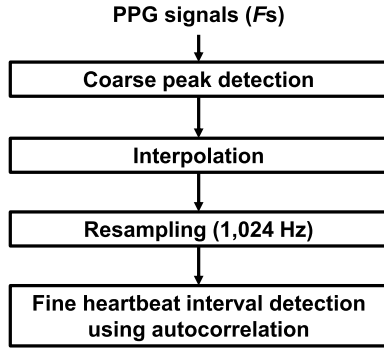


Fig. 3 Flowchart of heartbeat interval error compensation.

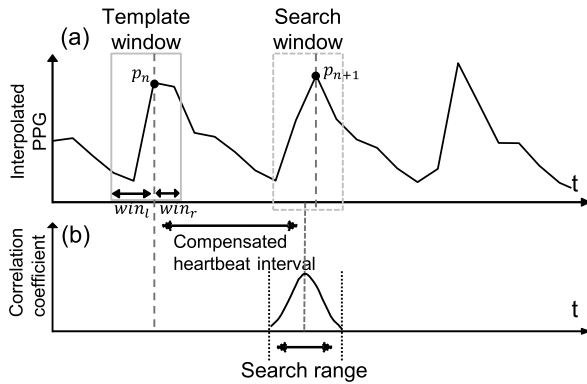


Fig. 4 Heartbeat interval error compensation technique using autocorrelation: (a) example of PPG wave and autocorrelation windows, (b) correlation coefficient used for compensated-peak determination.

those for which the sampling error is yet to be compensated (coarse peak detection). Finally, the peak is compensated using the autocorrelation of the waveform near the detected peak, as depicted in Fig. 4. The correlation operation is performed using the following Eq. (1):

$$\text{Cor}(s) = \sum_{i=-win_l}^{win_r} x(p_n + i)x(p_{n+1} + s + i) \quad (1)$$

Here,  $x$  is a zero-normalized input signal:  $p_n$  is a peak corresponding to the  $n$ -th period,  $win_l$ :  $win_r$  is the window size for autocorrelation; and  $s$  is the shift amount of the window. The search window and the template window are the same width, and the search window is shifted closer to the peak. Then, the point with the highest correlation coefficient, that is, the point with the highest similarity to the template window, is designated the compensated peak of the search window corresponding to the peak of the template window. The heartbeat interval is the length of the two peaks following compensation.

Figure 5(a) shows a comparison of the heartbeat intervals with and without the proposed error compensation method. Figure 5(b) shows the relative errors of the heartbeat interval that are calculated from the simultaneously measured reference ECG at a 1-kHz sampling rate. The accuracy of the heartbeat interval at 25-Hz  $F_s$  is sufficiently improved by the proposed method, compared to simple peak

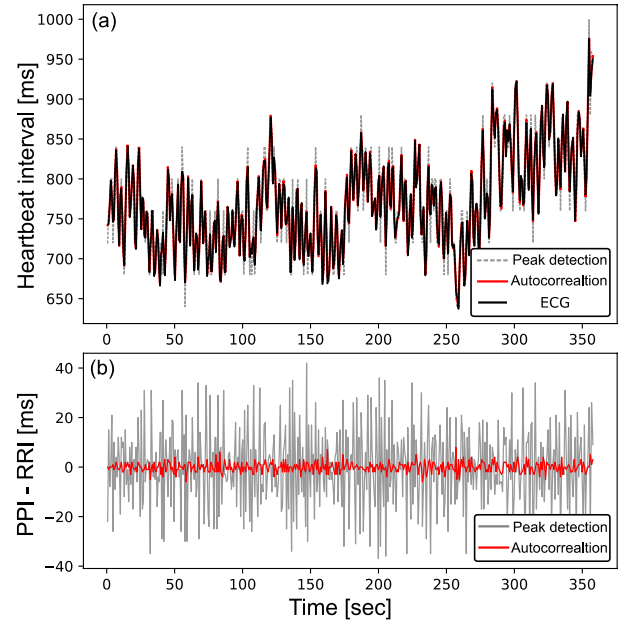


Fig. 5 Measured example of (a) heartbeat interval and (b) relative error compared with heartbeat interval from 1-kHz sampled ECG.

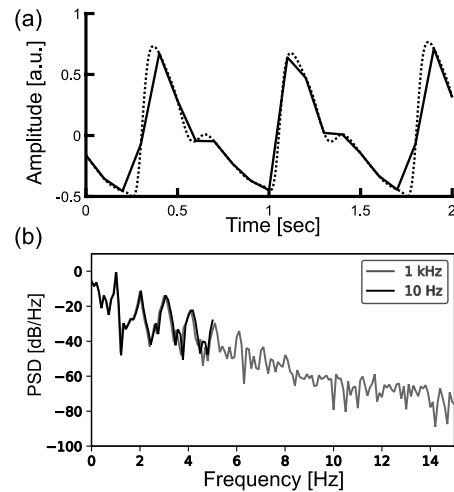


Fig. 6 (a) PPG waveforms and (b) the PPG power spectral density (PSD) at 1-kHz and 10-Hz sampling rate.

detection.

### 3.2 Waveform Similarity Improvement

Next, we introduce a waveform similarity improvement method using two-line approximation. Figure 6 shows the PPG waveform when 10-Hz  $F_s$  is superimposed on the 1-kHz PPG waveform and the PPG power spectral density (PSD). As shown in Fig. 6, waveform information such as peaks, is missing at ultra-low sampling rates. Furthermore, due to low waveform similarity, the proposed error compensation described in Sect. 3.1 is not sufficiently effective. Therefore, a pre-processing method for improving the waveform is required prior to error compensation using autocor-

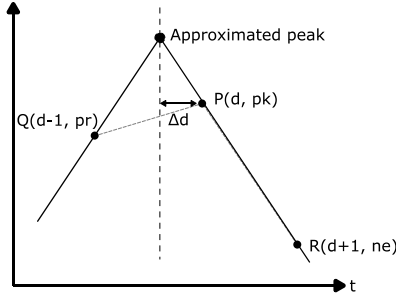


Fig. 7 Two-line approximation method.

relation.

In this study, pre-processing is performed using the two-line approximation, which can improve waveform similarity around peaks. Figure 7 illustrates the outline of this approximation algorithm. Here, we represent the coordinate of the peak as  $P(d, pk)$ , and the coordinates on both sides thereof as  $Q(d-1, pr)$ ,  $R(d+1, ne)$ . Then, the time distance of  $\Delta d$  between the detected peak and the new peak is expressed using the following Eq. (2):

$$\begin{aligned} \Delta d &= \frac{pr - ne}{2(ne - pk)} \quad (pr > ne) \\ \Delta d &= \frac{pr - ne}{2(pr - pk)} \quad (pr < ne) \end{aligned} \quad (2)$$

To apply this method to the compensation algorithm described in Sect. 3.1, the new peak obtained using this method and the original sampling point are linearly interpolated along the equiangular lines. Other sampling points besides the peak are interpolated as usual. When using a quadratic function for peak approximation, the  $\Delta d$  is expressed by the following Eq. (3):

$$\Delta d = \frac{pr - ne}{2(pr + ne) - 4pk} \quad (3)$$

### 3.3 Significance of Waveform Characteristics

In this section, we describe the significance of the PPG waveform characteristics on the proposed error compensation. In our preliminary study [15], heartbeat interval compensation algorithm using autocorrelation is applied to the ECG, which has sharper waveforms, compared with PPG (see Fig. 8). Figures 9 and 10 illustrate the correlation operation (1) for the artificial waveform examples assuming PPG and ECG, with and without superimposed noise. The correlation coefficient, calculated by (1), of the steep waveform changes sharply near the peak, while that of the smooth waveform changes gently. Thus, there is the possibility that the desired error compensation effect cannot be achieved due to noise in the situation.

Thus, the dependence of the error compensation efficiency of the proposed error compensation algorithm on the steepness of the peak waveform is a drawback. To mitigate this problem, we use the first derivative of PPG (FDPPG),

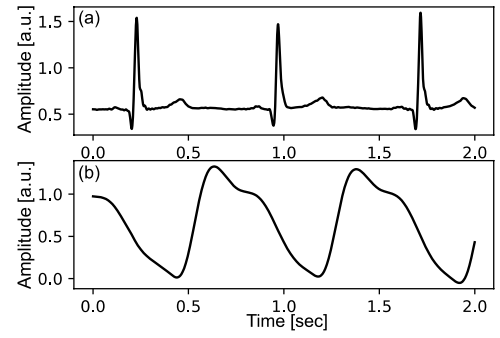


Fig. 8 Waveform examples: (a) ECG (b) PPG.

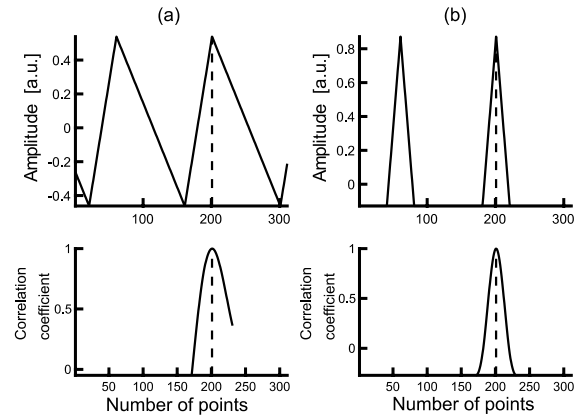


Fig. 9 Autocorrelation of artificial waves without noise: (a) smooth wave-like PPG, (b) steep wave-like ECG.

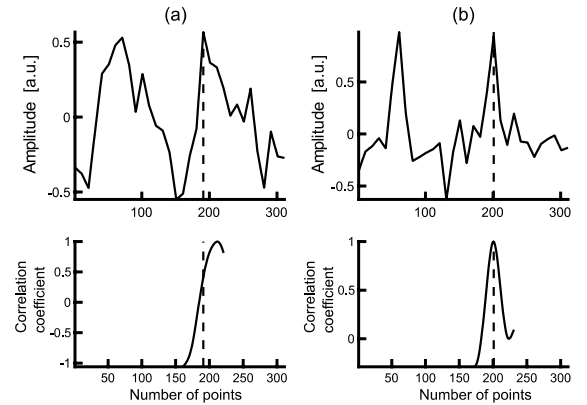
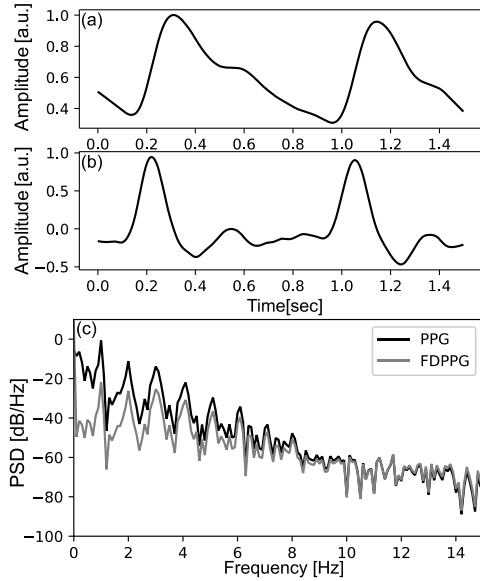


Fig. 10 Autocorrelation of artificial waves with noise: (a) smooth wave-like PPG, (b) steep wave-like ECG.

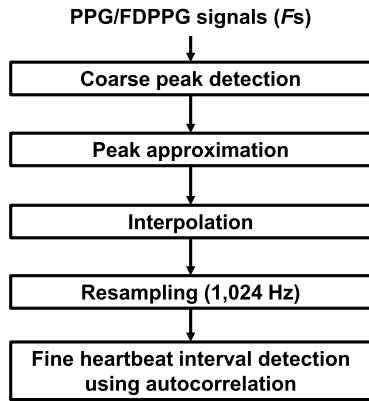
which has a steep change (see Fig. 11(b)). In addition, because the slope around the peak of FDPPG is symmetrical, the two-line approximation works effectively. Figure 11(c) shows the comparison between PPG and FDPPG PSDs.

Figure 12 illustrates a modified flowchart of heartbeat interval detection from Fig. 3 by adding the two-line approximation algorithm and FDPPG.





**Fig. 11** (a) PPG and (b) FDPPG waveforms and (c) the PSDs of PPG and FDPPG.



**Fig. 12** Flowchart of heartbeat interval error compensation with waveform similarity improvement methods.

## 4. Performance Evaluation

### 4.1 Evaluation Methods

To evaluate the performance of heartbeat interval error compensation, 360 seconds duration of PPG and ECG as a reference were synchronously measured from seven subjects (healthy, 21–24 years old male, at rest).

The mean absolute error (MAE) was used to evaluate the heartbeat interval error (4).

$$MAE = \frac{1}{n} \sum_{i=1}^n |PPI_i - RRI_i| \quad (4)$$

Here,  $RRI_i$  is the  $i$ -th heartbeat interval according to the ECG, and  $PPI_i$  is the  $i$ -th heartbeat interval according to the PPG.  $n$  is the number of data.

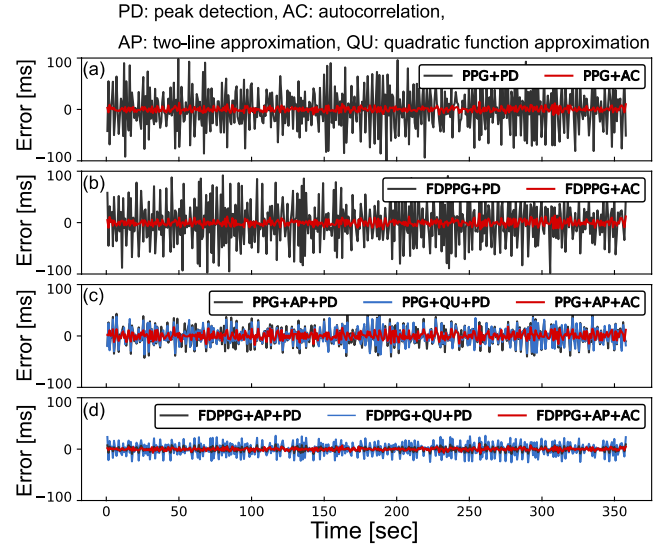


**Fig. 13** The heartbeat interval error at 10 Hz: (a) PPG, (b) FDPPG, (c) PPG and approximation and (d) FDPPG and approximation.

### 4.2 Heartbeat Interval

Figure 13 shows the comparison of the heartbeat interval error extracted by the conventional simple peak detection and the proposed error compensation using autocorrelation. Then, the sampling rate of PPG signal is set to 10-Hz  $F_s$ . PPG is used in Figs. 13(a) and (c), and FDPPG is used in Figs. 13(b) and (d). Figures 13 (c) and (d) show the results of applying each approximation method to Figs. 13(a) and (b). The combination of error compensation and approximation methods achieves minimum interval error.

Figure 14 shows the average MAE at each sampling rate for all the subjects. A combination of two-line approximation to the FDPPG and compensation using autocorrelation was characterized by less reduction in accuracy when the sampling rate is lowered to 10 Hz. When the sampling rate is 10 Hz, the MAE is 4.11 ms, and the accuracy degradation is only 0.52 ms with respect to the 1-kHz MAE. Figure 15 shows the MAE for each subject at the sampling rate of 10 Hz. The best MAE is exhibited by the autocorrelation method based on the two-line approximation to the FDPPG.

### 4.3 Heart Rate Variability (HRV) Analysis

In the HRV analysis, changes in heartbeat interval are analyzed in the time and frequency domains [3]. This result can be used for purposes such as heart disease detection and stress monitoring. In this paper, analysis in this study is dominantly performed in the frequency domain. The frequency analysis in the HRV spline interpolates the time series data of the heartbeat interval, and resamples at 4 Hz. Then, the sum of the power spectral density of the low-frequency component (LF) ranging from 0.04 Hz to 0.15 Hz and the high-frequency component (HF) ranging from 0.15 Hz to 0.40 Hz is calculated. The LF, HF, and

LF/HF are generally used as evaluation indexes.

The LF and HF reflect the sympathetic and parasympathetic nerve activities, respectively. Therefore, LF/HF represents the balance between the sympathetic and parasympathetic nerve activities. A high LF/HF denotes that the sympathetic nervous system has been activated, whereas a low LF/HF signifies that the parasympathetic nervous system has been activated.

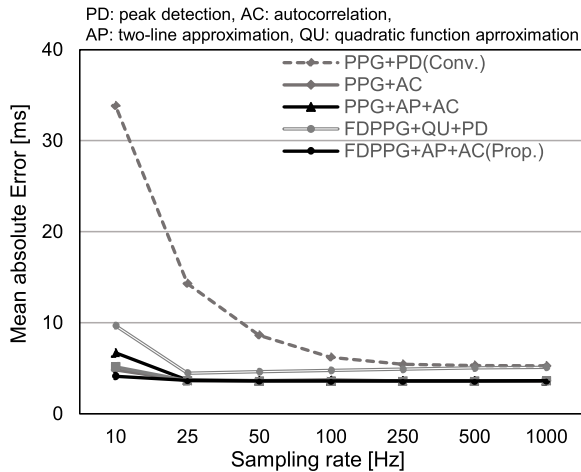


**Fig. 14** Relationship between MAE of heartbeat interval and sampling rates in each methods.

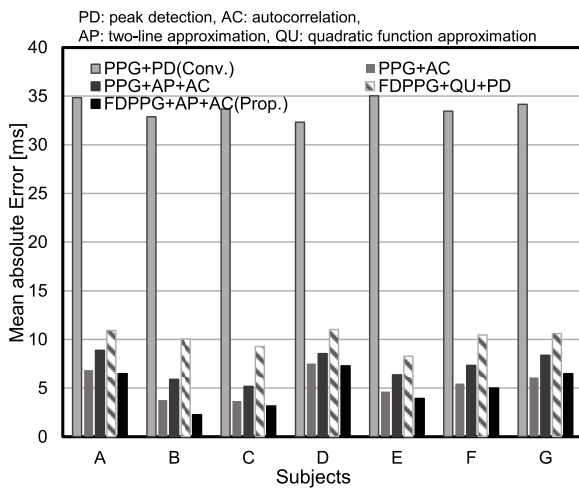


**Fig. 15** MAE comparison of each method and subject at 10 Hz.

Figure 16 shows a sample heartbeat interval and the corresponding result of the HRV analysis. The LF/HF in the heartbeat interval obtained from the ECG at 1 kHz and the PPG at 10 Hz are 1.482 and 0.612, respectively; a large error occurs if compensation is not performed. The LF/HF in the heartbeat interval determined using the autocorrelation of the FDPPG using a two-line approximation was 1.460. The very close results are attributed to the fact that the LF/HF obtained from the 1-kHz PPG is 1.520. Similarly, Table 1 shows the evaluation results of the LF/HF for each subject. Consequently, using the proposed method resulted in improved accuracy for all the subjects, and the mean absolute percentage error (MAPE) was reduced from 38.7% to 3.3%.

## 5. Discussion

The evaluation results in Sect. 4 suggest that the proposed method improves the accuracy at a low sampling rate. However, the peak approximation by the quadratic function at 10 Hz causes accuracy degradation. Nevertheless, the extent of accuracy degradation is reasonable, especially considering the fact that this method is inherently sensitive to noise,

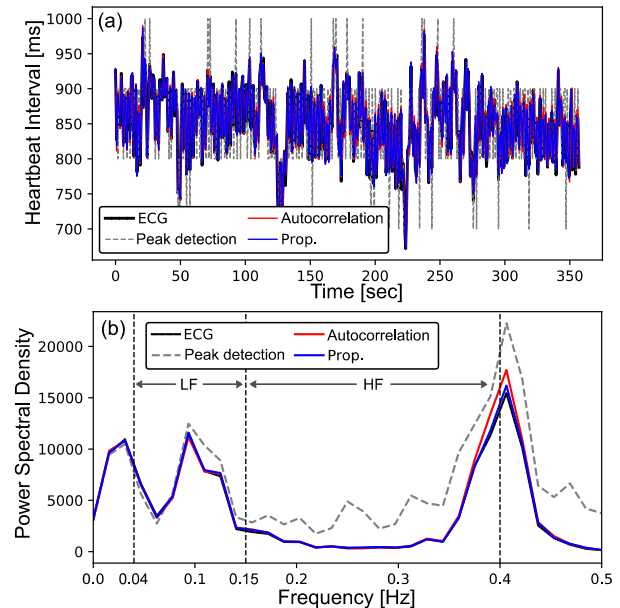


**Fig. 16** Examples of measured (a) heartbeat intervals and (b) HRV analysis result of frequency domain.

**Table 1** Comparison of LF/HF in each subject.

Subject	A	B	C	D	E	F	G
ECG at 1k Hz	1.176	0.637	1.887	1.676	0.346	1.482	0.208
Peak detection at 1k Hz	1.124	0.608	1.861	1.817	0.373	1.398	0.221
Peak detection at 10 Hz	0.660	0.374	1.363	0.705	0.246	0.612	0.234
Autocorrelation at 1k Hz	1.214	0.665	1.930	1.816	0.369	1.446	0.223
Autocorrelation at 10Hz	1.189	0.685	1.969	1.824	0.380	1.349	0.218
Prop. at 1k Hz	1.208	0.654	1.929	1.777	0.354	1.520	0.226
Prop. at 10 Hz	1.192	0.655	1.929	1.766	0.354	1.460	0.224



and such accuracy degradation is obtained at a low sampling rate where the signal-to-noise ratio reduces.

In HRV analysis, some subjects were slightly deteriorated in LF/HF although the accuracy was improved in MAE. This results may caused by the intrinsic difference of LF/HF between PPG and ECG [11], [20], [21].

In this study, we proposed a method that enables the accurate acquisition of heartbeat intervals using PPG at ultra-low sampling rates. This makes it possible to greatly reduce the activity rate of the LEDs, which although being a necessary portion of the PPG measurement, consume power significantly. To illustrate, a previous study [22] measures the PPG at sampling rate of 100 Hz, and found that the LED consumed the most power of all the components of the PPG sensor. By applying the proposed method toward similar end, the power consumption of the LED can be reduced by up to 1/10, that is, it can be reduced from 4400  $\mu$ W to 440  $\mu$ W.

Recently, an image PPG (iPPG) using a video camera for non-contact PPG measurement has also been proposed [23]. Because the frame rate of the video camera is generally limited, the proposed method can also be adopted and incorporated into the iPPG to improve the accuracy of the heartbeat interval. On the other hand, because the iPPG uses a non-contact sensor, various noises are easily superimposed on the results, and noise elimination becomes an important issue. Thus, it necessitates the incorporation of a noise removal algorithm, such as that in a prior study [24].

## 6. Conclusion

We proposed a sampling-rate reduction method based on linear interpolation and autocorrelation for heartbeat interval acquisition using PPG. By applying the proposed method, it is possible to reduce the activity rate of the circuits and LEDs in the PPG sensors, which can contribute to the reduction of power consumption. The results obtained using PPG show that it is possible to reduce the sampling rate to 10 Hz with a MAE of 4.11-ms through a pre-processing method based on two-line approximation and FDPPG. In the frequency analysis of the HRV, the LF/HF can be calculated with only 3.3% of the MAPE degradation at 10 Hz.

## References

- [1] Y. Han, M. Han, S. Lee, A.M.J. Sarkar, and Y.-K. Lee, "A framework for supervising lifestyle diseases using long-term activity monitoring," *Sensors (Basel)*, vol.12, no.5, pp.5363–5379, 2012.
- [2] S. Yazaki, "Evaluation of activity level of daily life based on heart rate and acceleration," *Proc. SICE Annu. Conf.* 2010, pp.1002–1005, 2010.
- [3] T. Kuusela, "Methodological aspects of heart rate variability analysis," *Heart Rate Variability (HRV) Signal Analysis*, pp.9–42, CRC Press, 2012.
- [4] R.W. DeBoer, J.M. Karemaker, and J. Strackee, "Comparing spectra of a series of point events particularly for heart rate variability data," *IEEE Trans. Biomed. Eng.*, vol.BME-31, no.4, pp.384–387, April 1984.
- [5] H.-G. Kim, E.-J. Cheon, D.-S. Bai, Y.H. Lee, and B.-H. Koo, "Stress and heart rate variability: A meta-analysis and review of the literature," *Psychiatry Investig.*, vol.15, no.3, pp.235–245, March 2018.
- [6] Muhadi, S.A. Nasution, R. Putranto, and K. Harimurti, "The ability of detecting heart rate variability with the photoplethysmography to predict major adverse cardiac event in acute coronary syndrome," *Acta Med. Indones.*, vol.48, no.1, pp.48–53, Jan. 2016.
- [7] Y. Athavale and S. Krishnan, "Biosignal monitoring using wearables: Observations and opportunities," *Biomed. Signal Process. Control*, vol.38, pp.22–33, Sept. 2017.
- [8] M. D and G. A, *Electrocardiography in Braunwald's Heart Disease*, 9th ed., Saunders, Philadelphia, 2012.
- [9] A.A.R. Kamal, J.B. Harness, G. Irving, and A.J. Mearns, "Skin photoplethysmography — A review," *Comput. Methods Programs Biomed.*, vol.28, no.4, pp.257–269, April 1989.
- [10] T. Tamura, Y. Maeda, M. Sekine, M. Yoshida, T. Tamura, Y. Maeda, M. Sekine, and M. Yoshida, "Wearable photoplethysmographic sensors—Past and present," *Electronics*, vol.3, no.2, pp.282–302, April 2014.
- [11] N. Selvaraj, A. Jaryal, J. Santhosh, K.K. Deepak, and S. Anand, "Assessment of heart rate variability derived from finger-tip photoplethysmography as compared to electrocardiography," *J. Med. Eng. Technol.*, vol.32, no.6, pp.479–484, Jan. 2008.
- [12] K. Matsumura, P. Rolfe, J. Lee, and T. Yamakoshi, "iPhone 4s photoplethysmography: Which light color yields the most accurate heart rate and normalized pulse volume using the iPhysioMeter application in the presence of motion artifact?," *PLoS One*, vol.9, no.3, p.e91205, March 2014.
- [13] J.P. Dieffenderfer, E. Beppler, T. Novak, E. Whitmire, R. Jayakumar, C. Randall, W. Qu, R. Rajagopalan, and A. Bozkurt, "Solar powered wrist worn acquisition system for continuous photoplethysmogram monitoring," 2014 36th Annual International Conference of the IEEE Engineering in Medicine and Biology Society, EMBC 2014, pp.3142–3145, 2014.
- [14] S. Rhee, B.-H. Yang, and H.H. Asada, "Artifact-resistant power-efficient design of finger-ring plethysmographic sensors," *IEEE Trans. Biomed. Eng.*, vol.48, no.7, pp.795–805, 2001.
- [15] Y. Nishikawa, S. Izumi, Y. Yano, H. Kawaguchi, and M. Yoshimoto, "Sampling rate reduction for wearable heart rate variability monitoring," *Proc. IEEE Int. Symp. Circuits Syst.*, vol.2018, May 2018.
- [16] P.K. Baheti and H. Garudadri, "An ultra low power pulse oximeter sensor based on compressed sensing," *Proc. 2009 6th International Workshop on Wearable and Implantable Body Sensor Networks*, BSN 2009, pp.144–148, 2009.
- [17] J. Lee, D.-H. Jang, S. Park, and S. Cho, "A low-power photoplethysmogram-based heart rate sensor using heartbeat locked loop," *IEEE Trans. Biomed. Circuits Syst.*, vol.12, no.6, pp.1220–1229, Dec. 2018.
- [18] H.J. Baek, J.W. Shin, G. Jin, and J. Cho, "Reliability of the parabola approximation method in heart rate variability analysis using low-sampling-rate photoplethysmography," *J. Med. Syst.*, vol.41, no.12, Dec. 2017.
- [19] K. Orth-Gomér, C. Hogstedt, L. Bodin, and B. Söderholm, "Frequency of extrasystoles in healthy male employees," *Br. Heart J.*, vol.55, no.3, pp.259–264, March 1986.
- [20] E. Gil, M. Orini, R. Bailón, J.M. Vergara, L. Mainardi, and P. Laguna, "Photoplethysmography pulse rate variability as a surrogate measurement of heart rate variability during non-stationary conditions," *Physiol. Meas.*, vol.31, no.9, pp.1271–1290, Sept. 2010.
- [21] M. Bolanos, H. Nazeran, and E. Haltiwanger, "Comparison of heart rate variability signal features derived from electrocardiography and photoplethysmography in healthy individuals," 2006 International Conference of the IEEE Engineering in Medicine and Biology Society, pp.4289–4294, Aug. 2006.
- [22] M. Tavakoli, L. Turicchia, and R. Sarpeshkar, "An ultra-low-power pulse oximeter implemented with an energy-efficient transimpedance amplifier," *IEEE Trans. Biomed. Circuits Syst.*, vol.4,

no.1, pp.27–38, Feb. 2010.

- [23] Y. Sun and N. Thakor, "Photoplethysmography revisited: From contact to noncontact, from point to imaging," *IEEE Trans. Biomed. Eng.*, vol.63, no.3, pp.463–77, March 2016.
- [24] M. Kumar, A. Veeraraghavan, and A. Sabharwal, "DistancePPG: Robust non-contact vital signs monitoring using a camera," *Biomed. Opt. Express*, vol.6, no.5, p.1565, May 2015.



**Kento Watanabe** received B.Eng. degrees in Computer Science and Systems Engineering from Kobe University, Kobe, Japan in 2018. He is currently in the master course at Kobe University. His current research is biomedical signal processing and low power sensor design.



**Shintaro Izumi** respectively received his B.Eng. and M.Eng. degrees in Computer Science and Systems Engineering from Kobe University, Hyogo, Japan, in 2007 and 2008. He received his Ph.D. degree in Engineering from Kobe University in 2011. He was a JSPS research fellow at Kobe University from 2009 to 2011, an Assistant Professor in the Organization of Advanced Science and Technology at Kobe University from 2011 to 2018, and an Associate Professor in the Institute of Scientific and Industrial Research at Osaka University from 2018 to 2019. Since 2019, he has been an Associate Professor in the Graduate School of System Informatics, Kobe University, Japan. His current research interests include biomedical engineering, biosignal processing, low-power circuit design, and sensor networks. He has served as a Technical Committee Member for IEEE Biomedical and Life Science Circuits and Systems, as a Student Activity Committee Member for IEEE Kansai Section, and as a Program Committee Member for IEEE Symposium on Low-Power and High-Speed Chips (COOL Chips). He was a Chair of IEEE Kansai Section Young Professionals Affinity Group and a recipient of 2010 IEEE SSCS Japan Chapter Young Researchers Award.



**Yuji Yano** received the M.S. degree in electronic engineering from the Hiroshima University, Hiroshima, Japan, in 2004. In 2004 he joined the SOC Division, Renesas Technology Corp., Hyogo, Japan. Since 2016, he has been a researcher at Graduate School of System Informatics, Kobe University, Hyogo, Japan, where he has been engaged in the design and development of the ultra-low power (ULP) system LSI solutions.



**Hiroshi Kawaguchi** received B.Eng. and M.Eng. degrees in electronic engineering from Chiba University, Chiba, Japan, in 1991 and 1993, respectively, and earned a Ph.D. degree in electronic engineering from The University of Tokyo, Tokyo, Japan, in 2006. He joined Konami Corporation, Kobe, Japan, in 1993, where he developed arcade entertainment systems. He moved to The Institute of Industrial Science, The University of Tokyo, as a Technical Associate in 1996, and was appointed as a Research Associate in 2003. In 2005, he moved to Kobe University, Kobe, Japan. Since 2007, he has been an Associate Professor with The Department of Information Science at that university. He is also a Collaborative Researcher with The Institute of Industrial Science, The University of Tokyo. His current research interests include low-voltage SRAM, RF circuits, and ubiquitous sensor networks. Dr. Kawaguchi was a recipient of the IEEE ISSCC 2004 Takuo Sugano Outstanding Paper Award and the IEEE Kansai Section 2006 Gold Award. He has served as a Design and Implementation of Signal Processing Systems (DISPS) Technical Committee Member for IEEE Signal Processing Society, as a Program Committee Member for IEEE Custom Integrated Circuits Conference (CICC) and IEEE Symposium on Low-Power and High-Speed Chips (COOL Chips), and as an Associate Editor of IEICE Transactions on Fundamentals of Electronics, Communications and Computer Sciences and IPSJ Transactions on System LSI Design Methodology (TSLDM). He is a member of the IEEE, ACM, IEICE, and IPSJ.



**Mashahiko Yoshimoto** joined the LSI Laboratory, Mitsubishi Electric Corporation, Itami, Japan, in 1977. From 1978 to 1983 he had been engaged in the design of NMOS and CMOS static RAM. Since 1984 he had been involved in the research and development of multimedia VLSI systems. He earned a Ph.D. degree in Electrical Engineering from Nagoya University, Nagoya, Japan in 1998. Since 2000, he had been a professor of Dept. of Electrical & Electronic System Engineering in Kanazawa University, Japan. Since 2004, he has been a professor of Dept. of Computer and Systems Engineering in Kobe University, Japan. His current activity is focused on the research and development of an ultra low power multimedia and ubiquitous media VLSI systems and a dependable SRAM circuit. He holds on 70 registered patents. He has served on the program committee of the IEEE International Solid State Circuit Conference from 1991 to 1993. Also he served as Guest Editor for special issues on Low-Power System LSI, IP and Related Technologies of IEICE Transactions in 2004. He was a chair of IEEE SSCS (Solid State Circuits Society) Kansai Chapter from 2009 to 2010. He is also a chair of The IEICE Electronics Society Technical Committee on Integrated Circuits and Devices from 2011–2012. He received the R&D100 awards from the R&D magazine for the development of the DISP and the development of the realtime MPEG2 video encoder chipset in 1990 and 1996, respectively. He also received 21th TELECOM System Technology Award in 2006.